Insect Biochemistry and Molecular Biology 109 (2019) 13–23

Contents lists available at ScienceDirect

Insect Biochemistry and Molecular Biology

journal homepage: www.elsevier.com/locate/ibmb

Small RNA responses of *Culex* mosquitoes and cell lines during acute and persistent virus infection

Claudia Rückert[a,*], Abhishek N. Prasad[a,b], Selene M. Garcia-Luna[a,c], Alexis Robison[a], Nathan D. Grubaugh[a,d], James Weger-Lucarelli[a,e], Gregory D. Ebel[a,**]

[a] Department of Microbiology, Immunology and Pathology, College of Veterinary Medicine and Biomedical Sciences, Colorado State University, Fort Collins, CO, 80523, USA
[b] Department of Pathology, Galveston National Laboratory, University of Texas Medical Branch, Galveston, TX, USA
[c] Department of Entomology, Texas A&M University, College Station, TX, USA
[d] Yale School of Public Health, Department of Epidemiology of Microbial Diseases, Laboratory of Epidemiology of Public Health, New Haven, CT, USA
[e] Department of Biomedical Sciences and Pathobiology, Virginia Polytechnic Institute and State University, Blacksburg, VA, USA

ARTICLE INFO

Keywords:
Mosquito
Culex
West nile virus
RNAi
Arbovirus
PIWI

ABSTRACT

RNA interference is a crucial antiviral mechanism in arthropods, including in mosquito vectors of arthropod-borne viruses (arboviruses). Although the exogenous small interfering RNA (siRNA) pathway constitutes an efficient antiviral response in mosquitoes, virus-derived P-element induced wimpy testis (PIWI)-interacting RNAs (piRNAs) have been implicated in the response to alpha-, bunya- and flaviviruses in *Aedes* spp. mosquitoes. *Culex* mosquitoes transmit several medically important viruses including West Nile virus (WNV), but are considerably less well studied than *Aedes* mosquitoes and little is known about antiviral RNA interference in *Culex* mosquitoes. Therefore, we sequenced small RNA (sRNA) libraries from different *Culex* cell lines and tissues infected with WNV. The clear majority of virus-derived sRNA reads were 21 nt siRNAs in all cell lines and tissues tested, with no evidence for a role of WNV-derived piRNAs. Additionally, we aligned sRNA reads from *Culex quinquefasciatus* Hsu cells to the insect-specific rhabdovirus, Merida virus, which persistently replicates in these cells. We found that a significant proportion of the sRNA response to Merida virus consisted of piRNAs. Since viral DNA forms have been implicated in siRNA and piRNA responses of *Aedes* spp. mosquitoes, we also tested for viral DNA forms in WNV infected *Culex* cells. We detected viral DNA in *Culex tarsalis* cells infected with WNV and, to a lesser amount, WNV and Merida virus-derived DNA in *Culex quinquefasciatus* Hsu cells. In conclusion, Hsu cells generated Merida virus-derived piRNAs, but our data suggests that the major sRNA response of *Culex* cells and mosquitoes to WNV infection is the exogenous siRNA response. It is also evident that sRNA responses differ significantly between specific virus-mosquito combinations. Future work using additional *Culex*-borne viruses may further elucidate how virus-derived piRNAs are generated in *Culex* cells and what role they may play in controlling replication of different viruses.

1. Introduction

The emergence and re-emergence of arthropod-borne viruses (arboviruses) (Vasconcelos and Calisher, 2016; Weaver and Reisen, 2010) such as West Nile virus (WNV) (Centers for Disease and Prevention, 1999; Kilpatrick, 2011), chikungunya virus (CHIKV) (Tsetsarkin et al., 2016) and Zika virus (ZIKV) (Lazear and Diamond, 2016; Weaver et al., 2016) demonstrates the significant risk arboviruses pose for global health. Vaccines are currently unavailable for most of these viruses and vector control remains a crucial yet problematic component of efforts to reduce virus transmission (Moyes et al., 2017). A more detailed understanding of molecular aspects of the virus-vector interaction could thus prove valuable to inform future strategies for the reduction of virus transmission, as shown previously with genetically modified mosquitoes (Alphey et al., 2013; Olson et al., 1996; Travanty et al., 2004; Winskill et al., 2015) or *Wolbachia* infected mosquitoes (Frentiu et al., 2014; McMeniman et al., 2009). *Culex* spp. mosquitoes are studied less than *Aedes* spp. mosquitoes despite their significance in transmitting medically important arboviruses such as WNV, St. Louis encephalitis virus and others currently circulating in the United States (Salimi et al.,

* Corresponding author.
** Corresponding author.
E-mail addresses: claudia.rueckert@colostate.edu (C. Rückert), gregory.ebel@colostate.edu (G.D. Ebel).

https://doi.org/10.1016/j.ibmb.2019.04.008
Received 4 December 2018; Received in revised form 1 April 2019; Accepted 2 April 2019
Available online 05 April 2019

2016).

In mosquitoes, arboviruses encounter immune responses including innate immunity signaling pathways and RNA interference (RNAi) (Rückert et al., 2014). While several signaling pathways have been implicated in antiviral responses in mosquito midguts and in cell culture (Carissimo et al., 2015; Fragkoudis et al., 2008; Paradkar et al., 2012; Ramirez and Dimopoulos, 2010; Souza-Neto et al., 2009; Xi et al., 2008), RNAi is generally considered the major antiviral defense mechanism in mosquitoes (Blair and Olson, 2015). The exogenous siRNA pathway has been implicated in mosquito antiviral defenses for over a decade (Adelman et al., 2002; Keene et al., 2004; Sanchez-Vargas et al., 2004). During virus infection of mosquito cells, the cytoplasmic RNase III enzyme Dicer-2 (Dcr2) recognizes viral replication intermediates in the form of long dsRNA molecules and cleaves them into fragments of predominantly 21bp length. These are incorporated into the RNA-induced silencing complex (RISC), where Argonaute-2 (Ago2) mediates cleavage of the target RNA using one of the strands (the 'guide strand'), while the complimentary strand (the "passenger strand") is discarded and degraded (Schwarz et al., 2003). Exogenous 21 nt virus-derived small interfering RNAs (vsiRNAs) are produced during arbovirus (Blair and Olson, 2015) and insect-specific virus infections (Carissimo et al., 2016; van Cleef et al., 2014), and it has been shown that arboviruses engineered to antagonize the mosquito exogenous RNAi pathway can cause increased mortality during infection (Cirimotich et al., 2009; Myles et al., 2008). RNAi is thus clearly critical to mosquito antiviral defenses. In recent years, the diversity of mosquito small RNA (sRNA) responses to arbovirus infections has become increasingly evident. Virus-derived piRNAs (vpiRNAs) are produced by *Aedes* mosquitoes and cells during infection with all major groups of arboviruses (Blair and Olson, 2015); however, of the seven *Aedes* PIWI proteins, only Piwi4 has been directly implicated in the control of virus replication (Schnettler et al., 2013) and this antiviral activity appears not to be mediated by vpiRNAs (Miesen et al., 2015; Schnettler et al., 2013; Varjak et al., 2017b).

Generally, piRNAs are important repressors of transposable elements (TEs), protecting the germline of a variety of organisms (Saito and Siomi, 2010; Senti and Brennecke, 2010; Siomi et al., 2010, 2011). Endogenous piRNAs originate from two distinct pathways. In the primary piRNA pathway, piRNAs are processed from single-stranded RNA precursors that are transcribed from genomic loci known as piRNA clusters. Primary piRNAs are typically antisense to TEs, exhibit a strong bias for a 5′-uridine residue (U_1), and, in *Drosophila*, are associated with the PIWI/Aubergine (Aub) protein complex (Nishida et al., 2007). Primary piRNAs are then fed into the second pathway, the "ping-pong dependent" amplification cycle. In this pathway, after binding of the target transcript, cleavage occurs ten nucleotides upstream from the 5′ end of the primary piRNA, resulting in secondary piRNAs with an adenine residue in position 10 (A_{10}), which are Argonaute-3 (Ago3) associated in *Drosophila* (Brennecke et al., 2007; Gunawardane et al., 2007). Secondary piRNAs then bind complementary targets resulting in cleavage at the A-U base-pairing, resulting in piRNAs identical (or very similar) to the initial primary piRNA, exhibiting a 5′-U_1 residue. Cleavage of the target transcript occurs via the Slicer activity of Ago3 in flies, but not mammals (Kim et al., 2009). The observed nucleotide bias is a hallmark of endogenous piRNAs, and is the basis for the ping-pong dependent amplification model (Brennecke et al., 2007; Gunawardane et al., 2007) which is also observed in other arthropods, including mosquitoes, and vertebrate germ line cells. The main difference in *Aedes* mosquitoes compared to *Drosophila melanogaster* is that mosquitoes have numerous PIWI genes (Ago3, Piwi1-7), four of which are also expressed somatically (Akbari et al., 2013). Piwi5, Piwi6 and Ago3 have been implicated in ping-pong amplification of transposon and Sindbis virus (SINV)-derived piRNAs in *Ae. aegypti* cells (Miesen et al., 2015), but the overall role of individual PIWI proteins in mosquitoes remains unclear.

In *Aedes* mosquitoes, vpiRNAs have been found not only in the ovaries and testes, but also in the mosquito bodies (Dietrich et al., 2017; Hess et al., 2011; Morazzani et al., 2012; Wang et al., 2018). One possible hypothesis for the generation of vpiRNAs in mosquitoes is linked to the control of persistent virus infection and tolerance in mosquitoes (Goic et al., 2016; Poirier et al., 2018). Recently, it has been suggested that viral DNA forms are generated by mosquito cells during virus infection (Goic et al., 2016; Nag et al., 2016a; Nag and Kramer, 2017). These viral DNA forms may serve as templates for vpiRNA generation, but are also important for generation of vsiRNAs (Goic et al., 2016; Poirier et al., 2018) as seen previously in persistent virus infection of *Drosophila* (Goic et al., 2013). While there are still many open questions regarding vpiRNA synthesis and their role in antiviral responses of *Aedes* spp. mosquitoes, RNAi responses of *Culex* spp. mosquitoes are comparatively understudied. Nonetheless, evidence for an exogenous RNAi response to WNV infection in *Culex quinquefasciatus* mosquitoes has been reported previously (Brackney et al., 2009; Fros et al., 2015; Göertz et al., 2016). Dietrich et al. (2017) further showed that *Cx. quinquefasciatus* can generate both vsiRNAs and vpiRNAs in response to Rift Valley fever virus (RVFV) infection.

In the present study, we characterized the sRNA responses of *Culex* mosquitoes and cell lines to WNV and two insect-specific viruses in order to assess whether vpiRNAs may be involved in antiviral responses of *Culex* mosquitoes. We sequenced sRNA libraries generated from WNV-infected *Culex* cells, mosquito midguts and salivary glands. As a comparison, we also sequenced sRNA libraries from midguts of WNV-infected *Ae. aegypti* mosquitoes, which are competent to transmit WNV but are not considered a vector species. We also quantified expression of putative PIWI pathway components in *Cx. quinquefasciatus* midguts and ovaries, as well as *Cx. quinquefasciatus* Hsu cells. Additionally, since insect-specific viruses are replicating persistently in both of our *Culex* cell lines, the flavivirus Calbertado virus (CLBOV) in *Culex tarsalis* CT cells (Aaron Brault, personal communication) and the rhabdovirus Merida virus (MERDV) in Hsu cells (Weger-Lucarelli et al., 2018), we also analyzed virus-derived small RNAs (vsRNAs) from these viruses. While we detected no vpiRNAs to CLBOV in CT cells, we found evidence for MERDV-derived piRNAs in Hsu cells. To investigate whether viral DNA forms are generated in *Culex* cells, we extracted DNA from virus-infected cell cultures and screened it for the presence of viral DNA. We found that viral DNA forms were produced by WNV-infected CT cells, but few WNV or MERDV DNA forms were detected in *Cx. quinquefasciatus* cells. Overall, we have characterized sRNA responses of *Culex* mosquitoes and cell lines to WNV, and we have shown that *Cx. quinquefasciatus* Hsu cells produce vpiRNAs derived from the rhabdovirus MERDV.

2. Materials and methods

2.1. Mosquitoes

Mosquito larvae of lab-colonized *Culex tarsalis*, strain KR83 (Eberle and Reisen, 1986), *Cx. quinquefasciatus* (Ciota et al., 2013) and *Ae. aegypti* from Chetumal, Mexico (Lozano-Fuentes et al., 2009), were raised on a diet of a 1:1 mix of powdered Tetra food and powdered rodent chow. Pupae were allowed to emerge into containers and adult mosquitoes were kept at 26–27 °C with a 16:8 light:dark cycle (*Culex* spp.) or a 12:12 light:dark cycle (*Ae. aegypti*) and 70%–80% relative humidity, with water and sugar provided ad libitum.

2.2. Cell lines

The *Cx. quinquefasciatus* ovary-derived cell line Hsu (Hsu et al., 1970) was maintained at 28 °C in DMEM supplemented with 10% FBS, 10% tryptose phosphate broth and antibiotics (100 units/mL penicillin and 100 μg/mL streptomycin) in a humidified atmosphere of 5% CO_2 in air. The *Cx. tarsalis*-derived embryonic cell line CT (Chao and Ball, 1976) was maintained at 28 °C in Schneider's *Drosophila* medium

supplemented with 10% FBS and antibiotics. The *Ae. albopictus*-derived embryonic cell line C6/36 (Singh, 1967) was maintained at 28 °C in EMEM supplemented with 10% FBS and antibiotics in a humidified atmosphere of 5% CO_2 in air.

2.3. Viruses

WNV was produced from an infectious clone based on the WNV_{NY99} strain of the virus as described elsewhere (Shi et al., 2002). Recombinant infectious-clone derived SINV strain MRE16 ($SINV_{5'dsMRE16}$icd) (Foy et al., 2004) was provided by Dr. Brian Foy (Colorado State University) and used to infect C6/36 cells as a positive control since we expected production of vpiRNAs from this virus-cell combination. The insect specific virus MERDV was found to infect Hsu cells by RNAseq (Weger-Lucarelli et al., 2018). The sequence of CLBOV was kindly provided by Dr. Aaron Brault (CDC, Fort Collins).

2.4. Virus infection of mosquitoes

Adult female mosquitoes 6–8 days post-eclosion were fed an infectious bloodmeal of defibrinated calf blood containing 1×10^8 PFU/mL of WNV_{NY99}icd and a final concentration of 2 mM ATP. Engorged mosquitoes were held for 7 or 14 days in a BSL-3 insectary under the same conditions as described above, after which they were cold anesthetized, and midguts and/or salivary glands were dissected and stored in miRvana RNA isolation lysis buffer (Ambion) at −80 °C until RNA isolation.

2.5. Virus infection of cell lines and viral growth curves

Hsu, CT and C6/36 cells were seeded in 24 well plates at a density of 3×10^5 cells/well and infected with WNV at MOI 5 or mock-infected by removal of media and incubation with 200 μL virus dilution in respective culture media supplemented with only 2% FBS. After 1 h, 1 mL regular culture media was added and the cells were incubated at 28 °C. For the growth curve, supernatant was collected every 24 h and cells were lysed every 24 h in TNA lysis buffer (Omega Bio-Tek) and stored at −80 °C. Infectious virus in the supernatant was titrated by standard plaque assay on Vero cells using an agar overlay. RNA from cell lysates was extracted using the Mag-Bind Viral DNA/RNA 96 kit (Omega Bio-Tek) on the KingFisher Flex Magnetic Particle Processor (Thermo Fisher Scientific). Viral RNA copies were quantified by qRT-PCR as previously described (Lanciotti et al., 2000).

2.6. Quantification of PIWI gene expression

In order to determine expression of PIWI genes in mosquito tissues and cell lines, RNA was extracted using the Mag-Bind Viral DNA/RNA 96 kit (Omega Bio-Tek) on the KingFisher Flex Magnetic Particle Processor (Thermo Fisher Scientific), DNase treated and cDNA was generated using the high capacity cDNA reverse transcription kit (Applied Biosystems). For mosquito tissues, PIWI genes and three house-keeping genes (18S rRNA, GAPDH and chymotrypsin) were then quantified by qPCR and PIWI expression was normalized to the three house-keeping genes. Since expression of GAPDH is stable in Hsu cells before and after infection (our own observation), only GAPDH was used as a housekeeping gene in qPCRs using Hsu cell cDNAs. All PCR primers are provided in Table S1.

2.7. Detection of viral DNA forms

DNA from cell lines and mosquito midguts was extracted using the Quick gDNA Miniprep kit (Zymo) according to the manufacturer's instructions. Samples were used directly for PCR or DNase treated using RQ1 DNase (Promega) for 30 min at 37 °C with subsequent DNase inactivation at 65 °C for 10min. Primers used for the detection of viral DNA forms are shown in Table S1 and Table S2.

2.8. Preparation of sRNA libraries and sequencing

Total RNA was extracted from homogenized mosquito midguts, salivary glands and cell lysates using the mirVana miRNA isolation kit (Ambion, Austin TX) as per manufacturer's instructions. RNA from individual midguts, salivary glands and cell culture samples were screened for the presence of WNV genomic RNA by 1-step RT-PCR (Qiagen, Valencia CA) using 1971-F (5′-TTGCAAAGTTCCTATCTCGT CAG-3′) and 2928c (5′-CCAAATCCAAAATCCTCCACTTCT-3′) primers. RNA quality of virus positive samples was determined using a 2100 Bioanalyzer (Agilent, Santa Clara CA). High quality, WNV positive midguts and salivary glands were then pooled into groups of five by tissue. Pooled RNA samples (and non-pooled cell culture samples) were precipitated by adding 3.25 vol of ice-cold ethanol, 0.1 vol 3M NaOAc (pH 5.5), and 1.5 μL of linear acrylamide (Ambion, 5 mg/mL). After overnight incubation at −20 °C, the pools were centrifuged at 20,000 g, washed twice with 80% EtOH, and re-suspended in 18uL nuclease-free water. For midguts and cell culture samples, 1 μg total RNA was used as the input for sRNA library preparation using the TruSeq Small RNA Sample Prep Kit (Illumina, San Diego CA) as per manufacturer's suggested protocol. Briefly, small RNAs were preferentially 3′ and 5′ adapter-ligated, reverse transcribed using the Superscript II reverse transcriptase (Invitrogen, Carlsbad CA), and PCR amplified, during which time a unique oligonucleotide barcode sequence was added to each library for multiplexing. Small RNA libraries were size selected on 2% TBE-agarose gels, and purified with MinElute Gel Extraction kits (Qiagen). Purified cDNA libraries were eluted in water, quality controlled on the 2100 Bioanalyzer, and sequenced on an Illumina HiSeq 2000 instrument (Beckman-Coulter Genomics). Salivary gland samples had extremely little input RNA (not detectable by Qubit high sensitivity RNA kit) and we found that library preparation using the Illumina TruSeq kit resulted in adapter dimer formation. Instead we used the NEBNext® Small RNA Library Prep Set for Illumina® to prepare libraries from salivary glands. We followed the manufacturer's instruction, but we diluted the 3′ and 5′ adapters 1:12 to allow for low input samples. We increased the number of cycles for the PCR amplification step to 24 cycles (recommended is 12–15) to allow visualization on a 2% agarose gel. We purified samples as described above and sequenced libraries on an Illumina NextSeq500 at the Colorado State University IDRC Genomics Core using 75 cycles of single read high output sequencing.

2.9. Analysis

The generated sRNA sequencing data (FASTQ files) were then analyzed using a pipeline established in our laboratory. Using the pipeline, FASTQ files were trimmed of the 3' adapter using FASTX Toolkit (http://hannonlab.cshl.edu/fastx_toolkit/), size selected (initially all 19–32 nt reads; then 19–23 nt and 24–32 nt) and aligned to the respective viral consensus sequence using Bowtie 0.12.8 (Langmead et al., 2009) allowing for 1-mismatch. The -a –best –strata mode was used, which instructs Bowtie to report only those alignments in the best alignment stratum. SAM output files produced by Bowtie were used as the input for processing through SAMtools (Li et al., 2009). From the individual read output, histograms were generated to show overall size and polarity distribution of vsRNA reads. Nucleotide targeting of the viral genome (i.e the number of vsRNA reads covering each nt position of the WNV genome) was determined using the mpileup function of SAMtools for 19–23 nt reads and 24–32 nt reads separately. Nucleotide bias of specific positions was analyzed and plotted using the R package viRome (Watson et al., 2013).

3. Results

3.1. Culex cells produce predominantly 21 nt siRNAs during acute and persistent WNV infection

We initially wanted to characterize sRNA responses of *Culex* cell lines after WNV infection. Accordingly, we established WNV replication and production kinetics in Hsu cells (*Cx. quinquefasciatus*), CT cells (*Cx. tarsalis*) and C6/36 cells (*Ae. albopictus*) after infection with MOI 5 (Fig. S1). From these kinetics, we decided to choose an early (2) and a late (6) day post infection (dpi) time point for our sRNA sequencing. Hsu cells, CT cells and C6/36 were either infected with WNV at MOI 5 or mock-treated and sRNA libraries were prepared from triplicate RNA samples at 2 and 6 dpi with WNV. C6/36 cells were used as a comparison in this experiment since they are derived from a non-*Culex* mosquito species (*Ae. albopictus*). As another technical control, C6/36 cells infected with SINV were included. Since we expected vpiRNA production in these cells following infection with SINV based on previous studies of SINV-derived sRNAs in *Aedes* cells (Brackney et al., 2010; Miesen et al., 2015; Vodovar et al., 2012), including them as a positive control would allow us to ensure that we can detect vpiRNAs with the methods used here for RNA extraction and library preparation. We also sequenced sRNA libraries from Hsu cells infected with WNV for 17 and 30 days (including several cell passages) to investigate sRNA responses during persistent WNV infection. No cytopathic effect (CPE) was observed in Hsu or CT cells at any point during virus infection. C6/36 cells showed CPE 6 dpi with WNV and 4 dpi with SINV.

In Hsu and CT cells infected with WNV, a strong vsRNA response was elicited (Table S2), generating almost exclusively 21 nt vsiRNAs at 2 dpi (Fig. S2A) and 6 dpi (Fig. 1A and B). We detected no obvious peak at any of the larger sRNA sizes (between 24 and 32 nt) that would be indicative of vpiRNAs. In order to assess whether vpiRNAs might be produced at lower levels, 24-32 nt sRNAs were analyzed for any positional nucleotide bias (such as U_1 or A_{10}); however, no strong bias was observed at any position (Fig. 1A and B). CT cells exhibited some bias for a U_1 (and U_2) of the antisense strand (Fig. 1B), but no signature of ping-pong amplification. No single 24–32 nt WNV-derived sRNA read was detected more than 74 times in any of the Hsu cell or CT cell samples. These data suggest that WNV-derived piRNAs are not produced during acute infection of *Culex* cells to a significant level.

In addition to acutely infected cells, we were also interested in vsRNA patterns during persistent infection. We infected Hsu cells with WNV, passaged infected cells for 17 and 30 dpi, extracted RNA and sequenced sRNA libraries. WNV RNA levels remained consistent at 17 and 30 dpi (Fig. S3) and we detected mostly 21 nt vsiRNAs with no evidence for vpiRNA production at 17 dpi (Fig. S2B) and 30 dpi (Fig. 2A). At 30 dpi, 24–32 nt vsRNAs had a random distribution along the WNV genome with no apparent strand (Fig. 2B) or nucleotide bias (Fig. 2A). Overall, WNV-derived sRNA reads from Hsu cells were comparable across all time points (2, 6, 17 and 30 dpi).

However, to exclude technical issues that may have resulted in this lack of vpiRNA detection, we next profiled sRNA reads from *Ae. albopictus* C6/36 cells infected with WNV and SINV. C6/36 cells are deficient in Dcr2 processing (Brackney et al., 2010) and generated predominantly 24–32 nt vsRNAs upon infection with both WNV (Fig. S4A) and SINV (Fig. S4B) by 6 dpi. Both WNV and SINV-infected cells had a vsRNA peak around 28 nt, with sRNA reads mainly derived from the positive strand; however, for SINV the peak was distinct, while WNV-infected cells generated a wider spectrum of sRNA of more variable length. Generally, SINV-infected C6/36 cells produced significantly

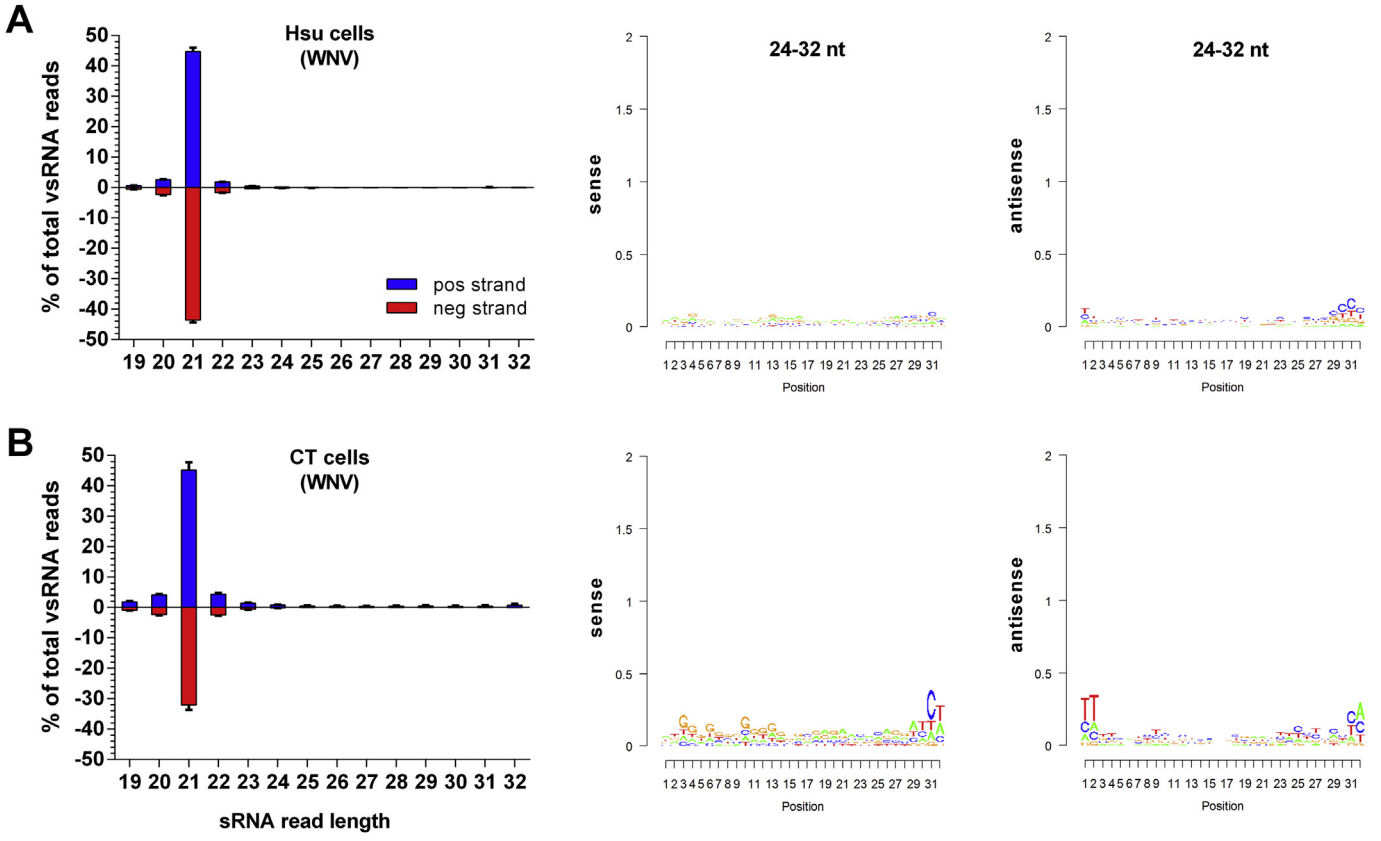

Fig. 1. Hsu and CT cells elicit a strong vsiRNA response to WNV infection. Profiling of vsRNAs aligning to WNV produced by Hsu cells (A) and CT cells (B) 6 dpi. Size distribution plots of sRNA reads are shown in the left panels. The mean from three replicate samples is shown and error bars indicate the range. Nucleotide bias of 24–32 nt sRNA reads derived from the sense and antisense genome is depicted in the middle and right panels, respectively. Data from one representative sample is shown.

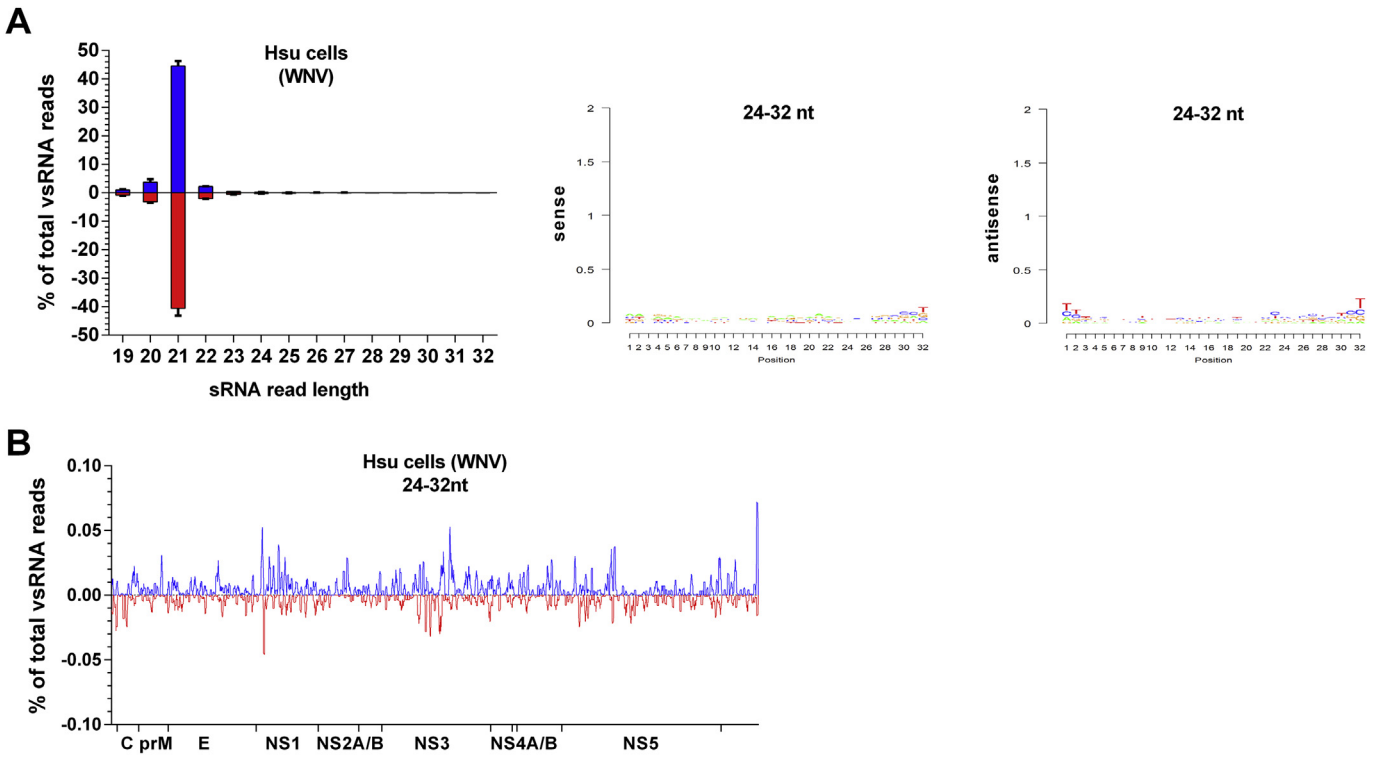

Fig. 2. WNV-derived sRNA profiles of persistently infected Hsu cells. Hsu cells were infected with WNV sRNA libraries sequenced 30 dpi. Size distribution plots of sRNA reads are shown in (A), left panel. The mean from three replicate samples is shown and error bars indicate the range. Nucleotide bias of 24–32 nt sRNA reads derived from the sense and antisense genome is depicted in the middle and right panels (A), respectively. Data from one representative sample is shown. Positional targeting of the WNV genome by 24–32 nt vsRNAs is shown in (B). Data represents the mean of three replicate samples.

more vsRNAs than WNV-infected C6/36 cells by 2 and 6 dpi (Table S3), with SINV-derived sRNAs making up 22.99% of all sRNA reads by 6 dpi. In comparison, only 1.55% of total sRNA reads were WNV-derived by 6dpi in WNV-infected C6/36 cells (Table S3). However, this observation may directly correlate with higher levels of SINV subgenomic RNA compared to WNV RNA which was not tested here. No signature of ping-pong amplification was found in 24–32 nt WNV-derived sRNAs, with no clear bias for a U_1 indicative of primary vpiRNAs (Fig. S4A). SINV-derived 24–32 nt sRNAs had a clear bias for a U_1 (T_1) in antisense derived sRNA reads and some bias for an A_{10} in sense sRNA reads, suggesting ping-pong amplification (Fig. S4B). WNV-derived 24–32 nt reads mapped predominantly to two specific loci along the WNV genome (Fig. S4C) – one in the region encoding NS5 (positions 10115–10142) and one at the very 3′UTR of the genome (positions 10999–11029). These positions were covered mainly by four individual sRNA reads, only one of which had a U_1 (T_1) (TGGTGGCTGGTGGTGC GAGAACACAGGATCT) while the other three had neither a U (T) at position 1 nor an A at position 10. However, we did not perform β-elimination assays in this study and cannot exclude that these reads may be vpiRNAs without the hallmark nucleotide bias as seen previously for flaviviruses in *Aedes* cells (Miesen et al., 2016; Scott et al., 2010; Varjak et al., 2017a). SINV-derived sRNA reads mapped more broadly along the 5′ end of the genome as well as the subgenomic RNA encoding the structural proteins (Fig. S4D). Our results from C6/36 cells provided evidence that our methods are suitable for the detection of vpiRNAs as shown for SINV-infected C6/36 cells.

3.2. *Culex quinquefasciatus* mosquito midguts and salivary glands predominantly generate 21 nt vsiRNAs upon WNV infection

We next wanted to focus on sRNA responses *in vivo* and analyzed the sRNA profiles of WNV-infected *Cx. quinquefasciatus* midguts and salivary glands. We chose these two tissues because they represent important barriers for virus dissemination and transmission in mosquitoes. Similar to our cell line experiment, we also included a non-vector species, *Ae. aegypti*, for comparison. We sequenced sRNA libraries generated from midguts and salivary glands of *Cx. quinquefasciatus* 7 and 14 dpi with WNV, respectively, as well as from midguts of *Ae. aegypti* mosquitoes 14 dpi with WNV. The numbers of 19–32 nt sRNA sequencing reads aligning to the WNV genome are shown in Table S3. In all samples, the predominant size of vsRNAs was 21 nt (Fig. 3, left panels), indicative of an exogenous siRNA response. In *Cx. quinquefasciatus* midguts (Fig. 3A) and salivary glands (Fig. 3B), there was no peak at any other read length that may be indicative of vpiRNAs.

WNV-infected *Ae. aegypti* midguts had two very small peaks at 26 nt and 28 nt length (Fig. 3C), potentially indicative of WNV-derived piRNA production. To determine whether vpiRNAs were present at low proportions, we analyzed 24-32 nt vsRNAs for any nucleotide bias indicative of primary (5′-U_1) or secondary (A_{10}) piRNAs. We observed no distinct nucleotide bias indicative of primary WNV-derived piRNAs or ping-pong amplification in any of the mosquito species/tissues. The small peaks at 26 and 28 nt length in *Ae. aegypti* midguts were directly caused by two dominating reads derived from the same region in NS5, CTGGCTGGGACACCCGCATCACGAGA(GC). These reads have an adenine at position 10 and may thus represent secondary piRNA reads, but no primary piRNA counterpart (sRNA beginning with the reverse complement of the first 10 nucleotides) was found at any read length (19–32 nt). Other studies of flaviviruses in *Aedes* mosquitoes and cell lines have found vpiRNAs derived from only a few regions along the genome lacking nucleotide bias (Miesen et al., 2016; Varjak et al., 2017a). One of these regions, highlighted by Varjak et al. (2017a), is mostly conserved in WNV, but we found no vpiRNA targeting this region in WNV.

In addition, we wanted to assess whether piRNAs can even be generated in *Cx. quinquefasciatus* midguts, and to further exclude the

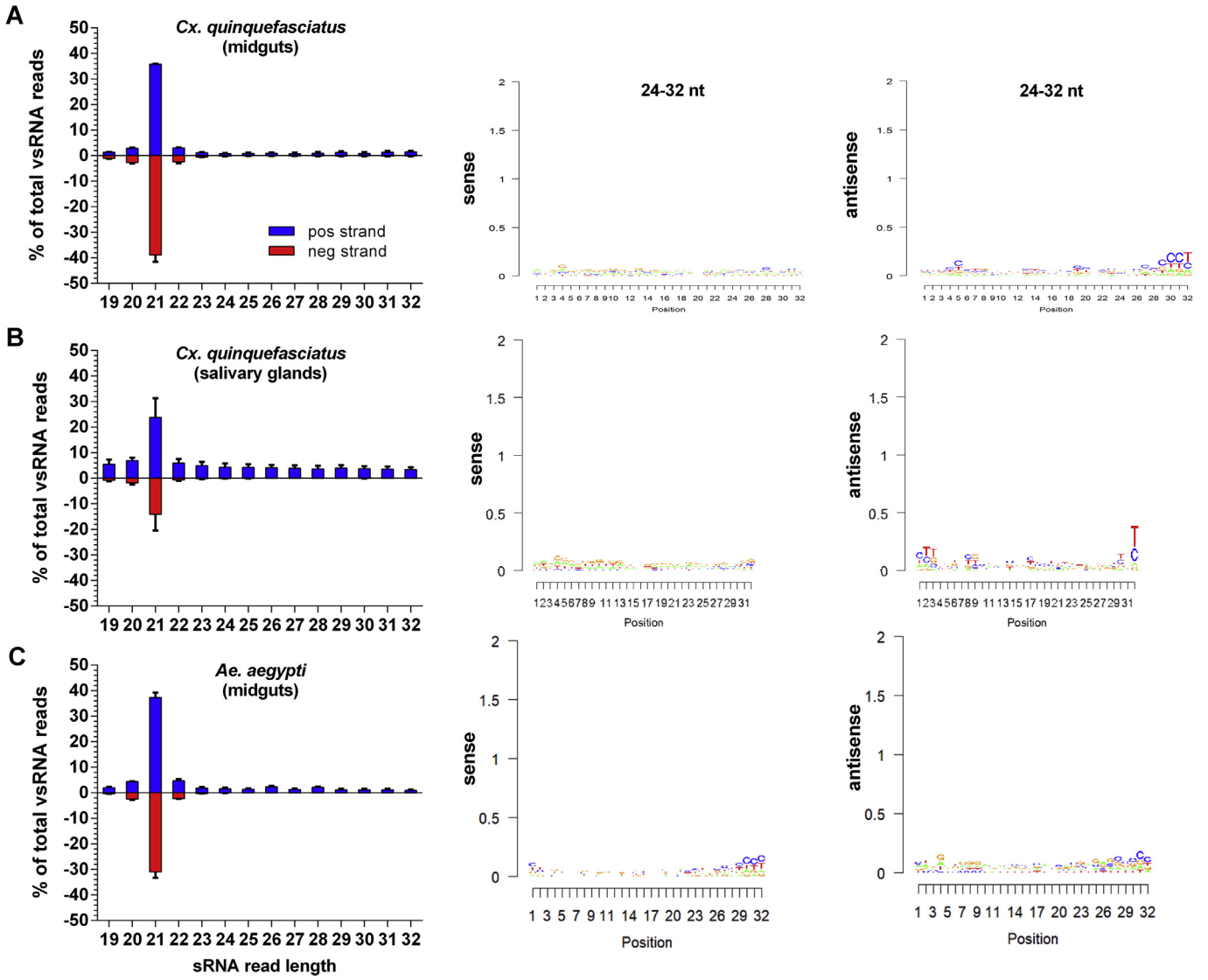

Fig. 3. WNV-derived sRNA profiles of mosquito midguts and salivary glands. sRNA libraries were sequenced from pools of five *Cx. quinquefasciatus* midguts 7 dpi with WNV (A) or pools of five *Cx. quinquefasciatus* salivary glands 14 dpi with WNV (B). sRNA libraries were also sequenced from pools of *Ae. aegypti* midguts 14 dpi with WNV (C). Mean sRNA read length from three combined replicates is shown in the left panels. Error bars indicate range. Read counts were normalized to the total number of reads and are shown as percent of total reads. Nucleotide bias of 24–32 nt sense reads (middle panels) and antisense (right panels) reads was analyzed using viRome (Watson et al., 2013). Data from one representative sample is shown for nucleotide bias analysis.

possibility that we lost piRNAs during library preparation. For this, we aligned our sRNA reads to two known retrotransposons found in the *Cx. quinquefasciatus* genome, Gypsy13 (Fig. S5A) and Gypsy1 (Fig. S5B). We identified sRNA reads of predominantly 24–28 nt length which aligned to the two retrotransposons. All sequences aligned to the negative strand of the retrotransposons and we observed a strong bias for a U_1 (T_1; Fig. S5), suggesting that these sequences correspond to primary piRNAs.

3.3. PIWI gene expression in Culex quinquefasciatus tissues and cells

To determine potential factors responsible for a lack of vpiRNAs in infected *Culex* midguts, we characterized PIWI gene expression in midguts and ovaries of *Cx. quinquefasciatus* mosquitoes. PIWI gene expression may indicate which genes are expressed in midguts and if any genes essential for ping-pong amplification, such as Ago3, are not expressed. Ovaries were used as a comparison since piRNAs are important for germ line protection and high expression of PIWI genes was thus anticipated in ovaries. We quantified relative gene expression of all PIWI genes and the accessory gene Zucchini (Zuc) in cDNA from three replicate pools of five midguts or five ovaries by qPCR. Expression was normalized to three housekeeping genes (GAPDH, chymotrypsin and 18S rRNA). While expression of all PIWI genes was high in ovaries and similar between genes, expression was generally lower in midguts and varied significantly between the different PIWI genes (Fig. 4A). Ago3, Piwi2, Piwi5 and Zuc were expressed at relatively high levels, but expression of Piwi6 was lower, and Piwi1, 3 and 4 were either below or just above the limit of detection of our assay (Fig. 4A). We also detected expression of PIWI genes in Hsu cells (Fig. 4B,C). Since virus infection often alters expression of selected genes, we were next interested in the impact of WNV infection on PIWI gene expression in *Culex* Hsu cells. To test whether virus infection of Hsu cells changes PIWI gene expression, cells infected with WNV were lysed at 2 dpi and 6 dpi and PIWI gene expression was determined by qRT-PCR. We did not detect any significant change in PIWI expression after WNV infection (Fig. 4B,C) at either time point (multiple unpaired t-tests with Holm-Sidak correction for multiple comparisons).

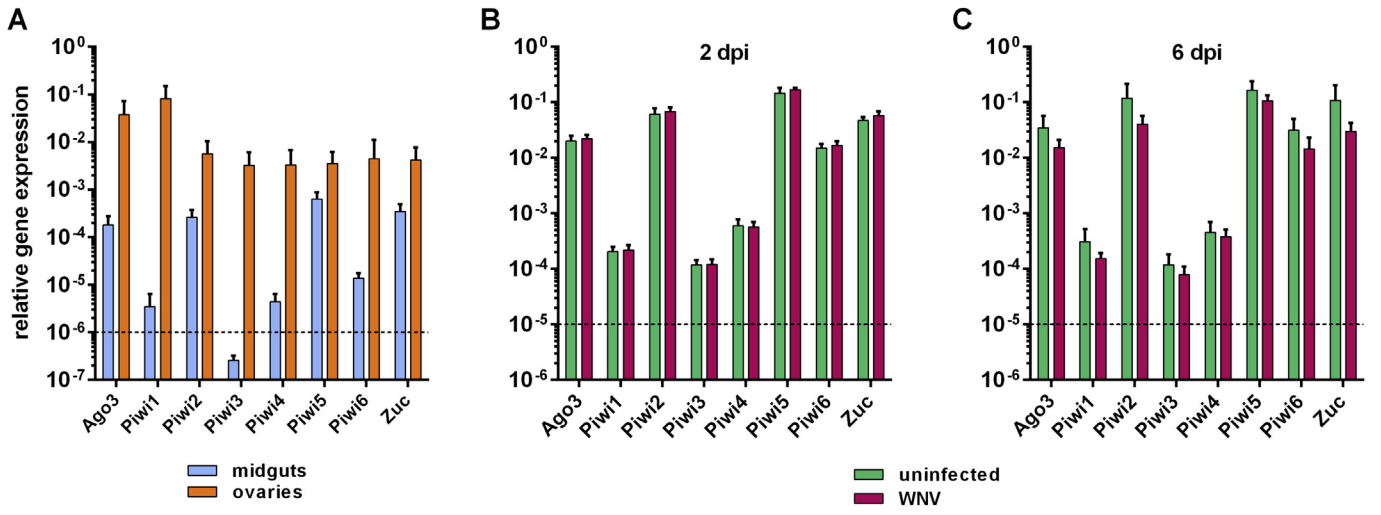

Fig. 4. PIWI gene expression in *Cx. quinquefasciatus* tissues and cells. Relative expression of individual key components of the PIWI pathway was determined in midguts and ovaries from *Cx. quinquefasciatus* (A) by qPCR and normalization to GAPDH, chymotrypsin and 18S rRNA. Error bars indicate standard deviation of 3 replicate pools of five midguts or five ovaries. The dotted line indicates the limit of detection and accurate quantification of our assay (corresponding to ct 36 in the qPCR). Expression of PIWI genes was also quantified in the *Cx. quinquefasciatus* cell line Hsu by qPCR and normalization to GAPDH at 2 dpi (B) and 6 dpi (C) with WNV. Error bars indicate standard deviation from 3 replicate samples. Statistical significance was calculated using multiple unpaired t-tests with Holm-Sidak correction for multiple comparisons.

3.4. Characterization of sRNAs derived from two insect-specific viruses replicating in Culex cells

After assessing sRNA profiles upon WNV infection, we were interested in the sRNA profiles derived from insect-specific viruses present in our cell lines. *Cx. tarsalis* CT cells are persistently infected with an insect-specific flavivirus, CLBOV (Aaron Brault, personal communication). Since we had sequenced sRNAs from mock-infected CT cells, we aligned sRNA reads from CT cells (2 days post mock-infection) to the genome of CLBOV to characterize the sRNA profile derived from this insect-specific flavivirus. Reads were mostly 21 nt in length and no strong evidence for vpiRNA reads was found (Fig. 5). Overall, the vsRNA profile was comparable to that of WNV-infected CT cells.

The discovery that MERDV persistently infects Hsu cells (Weger-Lucarelli et al., 2018) allowed us to further characterize the sRNA responses to this insect-specific rhabdovirus. We aligned 19–32 nt reads from mock-infected Hsu cells to the MERDV genome and plotted size distribution (Fig. 6A), distribution of reads along the genome (Fig. 6B,C) and nucleotide bias of 24–32 nt reads (Fig. 6D,E). Size distribution of reads aligning to MERDV was characterized by a distinct 21 nt peak, as well as a peak around 27 nt (Fig. 6A). 21 nt reads aligned both to the genome and antigenome of the virus, whereas 24-32 nt reads aligned predominantly to the positive sense RNA (antigenome). Positional targeting along the MERDV genome showed a striking bias for 21 nt reads at the 5‘ end of the genome (Fig. 6B), targeting both strands, whereas 24–32 nt vsRNA reads predominantly aligned to the positive strand (antigenome) at the 3’ end (Fig. 6C). Large areas of the viral genome were not targeted by vsRNAs. When we analyzed nucleotide bias in 24–32 nt vsRNAs, we observed a strong bias for an A_{10} (Fig. 6D) and a U_1 (Fig. 6E) (shown as T) of vsRNAs targeting the sense and antisense, respectively, suggesting ping-pong amplification of vpiRNAs in this virus-cell pairing. Another interesting observation was that 17 and 30 days post WNV infection of Hsu cells, no MERDV sRNA reads were detected above background levels (Table S2) which correlated with a lack of MERDV RNA in these samples (Fig. S3) suggesting MERDV was cleared during persistent WNV replication.

3.5. Production of viral DNA intermediates in Culex cells

It has been shown that DNA forms of arboviruses are generated in both *Drosophila* cells (Goic et al., 2013) and *Aedes* spp. mosquitoes *in vitro* and *in vivo* (Goic et al., 2016; Nag et al., 2016a; Nag and Kramer,

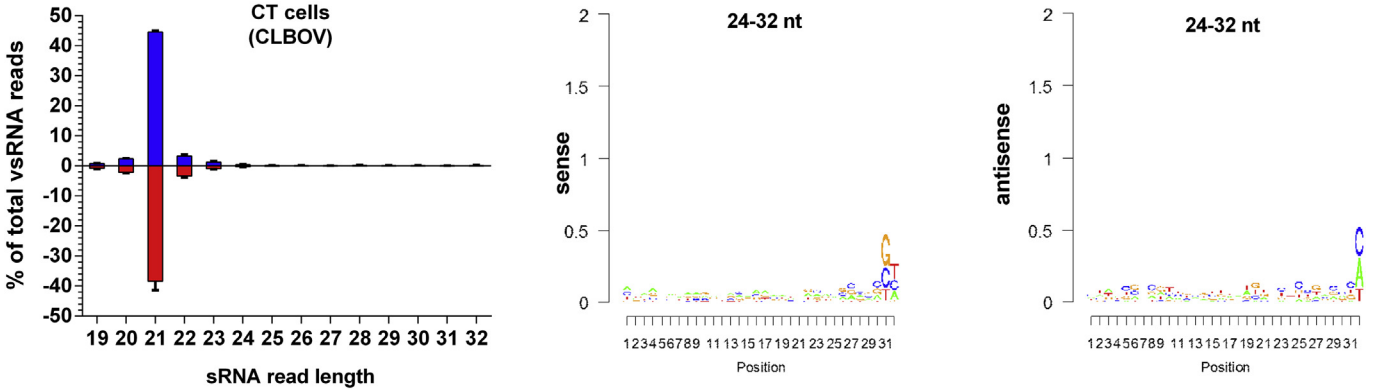

Fig. 5. CLBOV-derived sRNAs in *Cx. tarsalis* CT cells. sRNA libraries were sequenced from CT cells 2 days post mock-infection. Mean sRNA read length from three combined replicates is shown in the left panels. Error bars indicate range. Read counts were normalized to the total number of reads and are shown as percent of total reads. Nucleotide bias of 24–32 nt sense reads (middle panels) and antisense (right panels) reads was analyzed using viRome (Watson et al., 2013). Data from one representative sample is shown for nucleotide bias analysis.

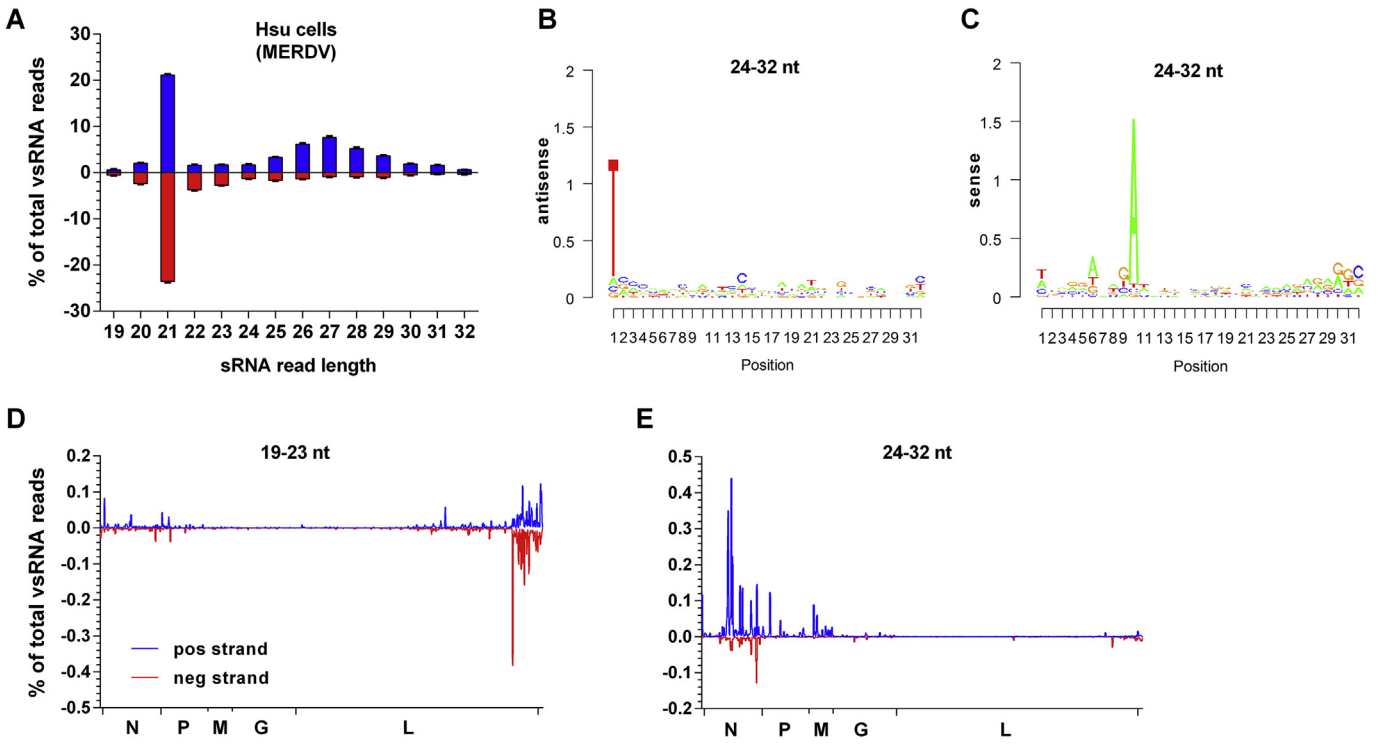

Fig. 6. Hsu cells produce vpiRNAs targeting MERDV. sRNAs isolated from three replicate cultures of Hsu cells persistently infected with MERDV were sequenced and profiled by size (A) and targeting along the virus genome of 19–23 nt reads (B) and 24–32 nt reads (C). Combined results from three replicate samples are shown. Nucleotide bias of 24–32 nt reads derived from the sense (D) and antisense (E) strand were analyzed using the R package viRome (Watson et al., 2013) and results from one representative sample are shown.

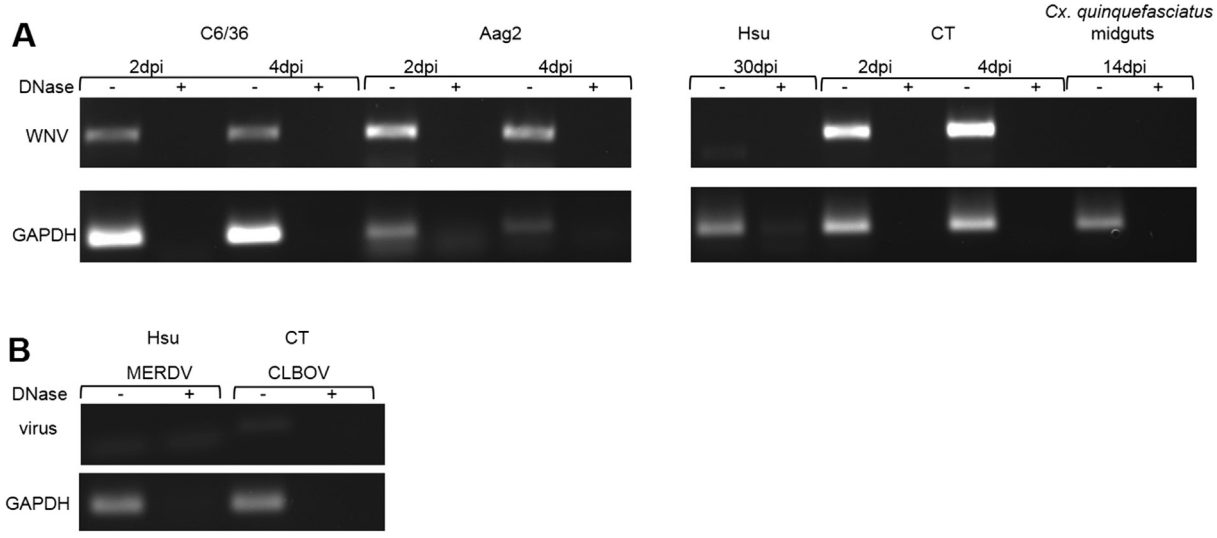

Fig. 7. WNV DNA forms are generated in C6/36, Aag2 and CT cells, but not Hsu cells. WNV PCRs were performed using template DNA extracted from C6/36, Aag2, Hsu and CT cells infected with WNV (A). WNV PCRs were also performed using DNA extracted from *Cx. quinquefasciatus* midguts 14 dpi with WNV (A). DNA was also extracted from Hsu and CT cultures which were not infected with WNV. This DNA was used to test for the presence of DNA forms of MERDV and CLBOV in Hsu and CT cells, respectively (B). A DNase treated negative control was included for all conditions, as well as a GAPDH positive control. PCRs were performed in triplicate samples; one representative sample is shown. Faint bands in Hsu cells are not of the correct size and represent primer dimers.

2017). Since these DNA forms are important for the generation of chikungunya virus derived siRNAs and piRNAs and mosquito tolerance in *Ae. albopictus* mosquitoes (Goic et al., 2016), we sought to determine whether *Culex* cells were also able to generate viral DNA forms. The *Culex* cell lines Hsu and CT, as well as the *Aedes* cell lines C6/36 and Aag2, were infected with WNV at MOI 1 and DNA was extracted 2 dpi, 4 dpi and for Hsu cells also 17 dpi and 30 dpi. As expected based on previous literature (Goic et al., 2016; Nag et al., 2016a; Nag and Kramer, 2017), viral DNA forms were observed in both C6/36 and Aag2 cell lines as early as 2 dpi (Fig. 7A). In CT cells, WNV DNA forms were also readily detected by 2 dpi. In *Cx. quinquefasciatus* Hsu cells we initially detected no viral DNA forms even by 30 dpi (Fig. 7A) using the selected WNV primer set (see Table S1) despite continuing virus replication (Fig. S3). Similarly, no viral DNA forms were detected in *Cx. quinquefasciatus* midguts 14 dpi with WNV (Fig. 7A).

To ensure that we did not miss viral DNA forms we next screened

Table 1
Detection of viral DNA forms in mosquito cells using primers along most of the genome.

Primer set[a]:		1	2	3	4	5	6	7	8	9	10	11	12	13	14	15	16	17	18	19	20	21	22	23	24
WNV	Aag2	+	+	+	+	+	+	+	+	+	-	+	+	+	+	+	+	+	+	+	+	+	+	+	+
	C6/36	+	+	+	+	+	+	+	+	+	+	+	+	+	+	+	+	+	+	+	+	+	+	+	+
	CT	+	+	+	+	+	+	+	+	-	-	+	+	+	+	+	+	+	+	+	+	+	+	+	+
	Hsu	-	-	+	+	-	+	-	+	-	-[b]	-	-	+	+	-	+	-	+	+	+	+	+	-	-[b]

Primer set[a]:		1	2	3	4	5	6	7	8	9	10	11	12	13	14	15	16	17	18	19	20	21	22	23	24	25	26	27	28
MERDV	Hsu	-	-	-	-	-	+	+	-[b]	-[b]	-	-	-	-	-	-	+	-	+	-	-	-	-[b]	-	-	-	-	-	-

[a] For distribution of primer sets along WNV and MERDV genomes, see Table S2.
[b] Faint bands of a correct/nearly correct size were detected but were found to be cellular *Cx. quinquefasciatus* genes upon Sanger sequencing.

DNA from WNV-infected Aag2 cells (4 dpi), C6/36 cells (4 dpi), CT cells (4 dpi) and Hsu cells (17 dpi) using 24 primer sets binding along almost the entire WNV genome (for primers see Table S2). In Aag2, C6/36, and CT cells most or all regions of the genome were detected as DNA forms (Table 1). In Hsu cells, detection of WNV DNA was sporadic, but multiple genome regions were detected in at least one of three replicate DNA samples at 17 dpi (Table 1; Fig. S6). Only one region along the WNV genome was detected in all three replicate samples tested (primer set 21, amplifying a region of NS5).

We were also interested in determining whether viral DNA forms are generated from persistent insect-specific viruses in *Culex* cells. We thus screened DNA extracted from untreated Hsu and CT cells for MERDV DNA and CLBOV DNA, respectively (Fig. 7B). No MERDV DNA was detected in our initial screen, but a faint signal of CLBOV DNA was detected in CT cells. We next used 28 primer sets amplifying along the MERDV genome to detect if any DNA forms were present (for primers see Table S2). For any PCR products of roughly the correct size, sanger sequencing was performed to confirm a viral origin. We found only four primer sets (Table 1) that amplified a WNV-confirmed PCR product from at least one replicate Hsu DNA sample. These primers did not amplify a region with significant vpiRNA production. These data suggest that while Hsu cells can generate viral DNA forms, this may occur at a lower frequency than in other mosquito cell lines. However, this lack of abundant viral DNA forms may be associated with relatively low levels of WNV and MERDV RNA in Hsu cells (Fig. S1 and Fig. S3). Overall, we found little evidence for viral DNA forms of genome regions heavily targeted by vpiRNAs (primer sets 1–5).

4. Discussion

In the present study, we characterized vsRNA responses of *Culex* mosquito tissues and cell lines to acute infection with WNV and persistent infection with WNV and two insect-specific viruses. Overall, we found that *Culex* midguts, salivary glands and cell lines generated a strong exogenous siRNA response to WNV, but no significant levels of vpiRNAs were detected. The vsRNA profiles were comparable between acute and persistent WNV infection in *Culex* cells, and sRNA size distribution was comparable in *Cx. tarsalis* cells infected with the insect-specific flavivirus CLBOV. In contrast, we detected a peak of 28 nt sRNA reads in SINV-infected C6/36 cells with the classic hallmark nucleotide bias (U_1/A_{10}) indicative of ping-pong amplification. We also detected a less distinct peak at 28 nt in WNV-infected C6/36, but without a clear nucleotide bias as shown previously for flavivirus-derived piRNAs in *Aedes* mosquito cells (Miesen et al., 2016; Varjak et al., 2017a). Together these data indicate that piRNAs may not be generated by *Culex* cells upon flavivirus infection. While additional viruses and mosquito tissues should be tested in the future, our inability to detect vpiRNAs in mosquito midguts and salivary glands indicates that it is unlikely that vpiRNAs significantly impact flavivirus transmission through antiviral function. Instead, products of the siRNAs appear to be the only sRNAs with the potential to impact virus transmission in *Culex* mosquitoes under natural conditions.

It may be that vpiRNAs were lost during sRNA library preparation due to an unidentified technical factor. However, since we detected piRNAs in samples that were sequenced in parallel and prepared by the same methods (SINV-infected C6/36 cells, MERDV-infected Hsu cells, retrotransposons in midguts), this possibility seems unlikely. Another technical limitation may have been sequencing depth. Sequencing depth of vsRNA reads was relatively low in WNV-infected *Cx. quinquefasciatus* midguts (Table S3); however, since we had good sequencing depth in our cell line samples and a lack of vpiRNAs in WNV-infected *Culex* mosquitoes has previously suggested (Brackney et al., 2009; Fros et al., 2015; Göertz et al., 2016), we are confident that *Culex* mosquitoes do not generate any significant amount of WNV-derived piRNAs. In comparison, we found only one predominant sRNA sequence of 26–28 nt length that may be indicative of a vpiRNA in WNV-infected *Ae. aegypti* midguts. This sRNA had no classic piRNA nucleotide bias. It has previously been shown that flavivirus-derived piRNAs in *Ae. aegypti* cells target few selected regions and have no nucleotide bias, as seen for DENV (Miesen et al., 2016) and ZIKV (Varjak et al., 2017a). However, we did not find vpiRNAs derived from same region in NS5 as for DENV and ZIKV in these studies (highlighted by Varjak et al., 2017a,b).

While we did not find any strong evidence for WNV-derived piRNAs in *Culex* tissues or cells, we did detect piRNAs derived from an insect-specific rhabdovirus, MERDV, which persistently infects *Cx. quinquefasciatus* Hsu cells. This finding and recent work showing that *Cx. quinquefasciatus* mosquitoes generate vpiRNAs targeting RVFV (Dietrich et al., 2017), indicate that *Culex* mosquitoes have the capability to produce vpiRNAs. However, vpiRNAs from these mosquitoes may be generated from negative sense, but not positive sense RNA viruses. While further evidence is needed to confirm this observation on a larger scale, sRNA responses clearly differ among these specific virus-mosquito pairings.

We also investigated whether the lack of vpiRNAs in *Culex* mosquitoes may be linked to PIWI gene expression. We detected expression of all known PIWI genes in *Cx. quinquefasciatus* ovaries and high expression of Ago3, Piwi2, Piwi5 and Piwi6 in *Cx. quinquefasciatus* midguts. However, expression of Piwi1, Piwi3 and Piwi4 was significantly lower in midguts. This is in accordance with PIWI expression in *Ae. aegypti*, where Piwi1-3 are germline specific (Akbari et al., 2013). It is important to note that there is a discrepancy in labeling between mosquito PIWI genes - *Cx. quinquefasciatus* Piwi4 appears to be a direct orthologue of *Ae. aegypti* Piwi2, while *Cx. quinquefasciatus* Piwi2 is most closely related to *Ae. aegypti* Piwi6 (Campbell et al., 2008) and appears to be a paralog of *Cx. quinquefasciatus* Piwi6. Expression of PIWI genes was comparable between midgut tissues and Hsu cells, despite the ovarian origin of Hsu cells. Importantly, we detected piRNAs derived from MERDV in Hsu cells, despite low level expression of Piwi1, Piwi3 and Piwi4 in these cells. This observation suggests that vpiRNA production may be mediated by Ago3, Piwi2, Piwi5 and/or Piwi6 in *Culex* cells. Further studies using gene silencing approaches will be necessary to identify the specific molecules that produce vpiRNAs in *Culex* mosquitoes. Notably, vpiRNA production has been associated with Ago3,

Piwi5 and Piwi6 in *Ae. aegypti* cells (Miesen et al., 2015, 2016).

Recent research has highlighted the significance of viral DNA forms generated by *Drosophila* and *Aedes* mosquito cells for the establishment of persistent infections (Goic et al., 2013, 2016). In *Aedes* mosquito cells, viral DNA forms of arboviruses are generated rapidly upon infection (Goic et al., 2016; Nag et al., 2016b; Nag and Kramer, 2017). Both circular and linear viral DNA is generated in a Dicer-2-dependent manner, presumably from defective genomes (Poirier et al., 2018). These viral DNA forms seem to serve as templates for vsiRNA and vpiRNA production in *Aedes* mosquitoes, as AZT treatment, which blocks reverse transcription of viral RNA into DNA, reduces overall numbers of vsiRNA and vpiRNA reads (Goic et al., 2016). AZT treatment also reduced mosquito survival following infection, suggesting that viral DNA forms are critical mediators of infection tolerance (Goic et al., 2016). While we observed viral DNA forms in WNV infected *Cx. tarsalis* cells (CT) and WNV-infected *Cx. quinquefasciatus* cells (Hsu), we found little evidence for MERDV-derived DNA forms in Hsu cells. Only four short segments of the genome could be detected as DNA forms. WNV DNA forms in Hsu cells were also harder to detect and only a few regions of the genome were represented, varying between replicates. However, since the generation of viral DNA forms in *Drosophila* has been shown to be driven by circulating hemocytes in order to mediate a systemic sRNA response (Tassetto et al., 2017), viral DNA forms may be produced more readily in other cell types of *Cx. quinquefasciatus* that we did not investigate here. The absence of MERDV DNA of regions targeted by MERDV-derived vpiRNAs in Hsu cells, however, may suggest that viral DNA forms may not be required for the production of vpiRNAs in these cells. Interestingly, the lack of abundant viral DNA forms in *Cx. quinquefasciatus* cells upon virus infection may explain previous observations that the *Cx. quinquefasciatus* genome contains less integrated viral elements than *Aedes* spp. genomes (Palatini et al., 2017).

In conclusion, we have characterized sRNA responses of *Culex* cells and mosquitoes to acute and persistent WNV infection, as well as to two insect-specific viruses. We found that the exogenous siRNA response may be the only sRNA response to WNV infection in *Culex* cells and mosquitoes. In contrast, vpiRNAs were generated from the insect-specific rhabdovirus MERDV in *Culex* cells. Future work should aim at elucidating the molecular mechanisms of vpiRNA production in *Culex* mosquitoes as it is evident that there are differences compared to *Aedes* mosquitoes, which may influence vector competence, virus persistence and virus-mosquito interactions.

Declarations of interest

The authors declare no conflicts of interest.

Acknowledgments

The authors would like to thank Dr. Aaron Brault, Centers for Disease Control and prevention, for providing Hsu cells, CT cells, and the Calbertado virus sequence. The mosquito used in the graphical abstract was provided by Ana L. Ramírez through figshare (Ramírez, 2019). This study was funded by NIH grant AI067380.

Appendix A. Supplementary data

Supplementary data related to this article can be found at https://doi.org/10.1016/j.ibmb.2019.04.008.

References

Adelman, Z.N., Sanchez-Vargas, I., Travanty, E.A., Carlson, J.O., Beaty, B.J., Blair, C.D., Olson, K.E., 2002. RNA silencing of dengue virus type 2 replication in transformed C6/36 mosquito cells transcribing an inverted-repeat RNA derived from the virus genome. J. Virol. 76, 12925–12933.

Akbari, O.S., Antoshechkin, I., Amrhein, H., Williams, B., Diloreto, R., Sandler, J., Hay, B.A., 2013. The developmental transcriptome of the mosquito Aedes aegypti, an invasive species and major arbovirus vector. G3 (Bethesda) 3, 1493–1509.

Alphey, L., McKemey, A., Nimmo, D., Neira Oviedo, M., Lacroix, R., Matzen, K., Beech, C., 2013. Genetic control of *Aedes* mosquitoes. Pathog. Glob. Health 107, 170–179.

Blair, C.D., Olson, K.E., 2015. The role of RNA interference (RNAi) in arbovirus-vector interactions. Viruses 7, 820–843.

Brackney, D.E., Beane, J.E., Ebel, G.D., 2009. RNAi targeting of West Nile virus in mosquito midguts promotes virus diversification. PLoS Pathog. 5, e1000502.

Brackney, D.E., Scott, J.C., Sagawa, F., Woodward, J.E., Miller, N.A., Schilkey, F.D., Mudge, J., Wilusz, J., Olson, K.E., Blair, C.D., et al., 2010. C6/36 Aedes albopictus cells have a dysfunctional antiviral RNA interference response. PLoS Neglected Trop. Dis. 4, e856.

Brennecke, J., Aravin, A.A., Stark, A., Dus, M., Kellis, M., Sachidanandam, R., Hannon, G.J., 2007. Discrete small RNA-generating loci as master regulators of transposon activity in *Drosophila*. Cell 128, 1089–1103.

Campbell, C.L., Black, W.C.t., Hess, A.M., Foy, B.D., 2008. Comparative genomics of small RNA regulatory pathway components in vector mosquitoes. BMC Genomics 9, 425.

Carissimo, G., Eiglmeier, K., Reveillaud, J., Holm, I., Diallo, M., Diallo, D., Vantaux, A., Kim, S., Menard, D., Siv, S., et al., 2016. Identification and characterization of two novel RNA viruses from *Anopheles gambiae* species complex mosquitoes. PLoS One 11, e0153881.

Carissimo, G., Pondeville, E., McFarlane, M., Dietrich, I., Mitri, C., Bischoff, E., Antoniewski, C., Bourgouin, C., Failloux, A.B., Kohl, A., et al., 2015. Antiviral immunity of *Anopheles gambiae* is highly compartmentalized, with distinct roles for RNA interference and gut microbiota. In: Proceedings of the National Academy of Sciences of the United States of America. 112. pp. E176–E185.

Centers for Disease, C., Prevention, 1999. Outbreak of West Nile-like viral encephalitis–New York, 1999. MMWR Morb. Mortal. Wkly. Rep. 48, 845–849.

Chao, J., Ball, G.H., 1976. A comparison of amino acid utilization by cell lines of *Culex tarsalis* and *Culex pipiens*. In: Invertebrate Tissue Culture: Applications in Medicine, Biology, and Agriculture, pp. 263–266.

Ciota, A.T., Chin, P.A., Kramer, L.D., 2013. The effect of hybridization of Culex pipiens complex mosquitoes on transmission of West Nile virus. Parasites Vectors 6, 305.

Cirimotich, C.M., Scott, J.C., Phillips, A.T., Geiss, B.J., Olson, K.E., 2009. Suppression of RNA interference increases alphavirus replication and virus-associated mortality in *Aedes aegypti* mosquitoes. BMC Microbiol. 9, 49.

Dietrich, I., Jansen, S., Fall, G., Lorenzen, S., Rudolf, M., Huber, K., Heitmann, A., Schicht, S., Ndiaye, E.H., Watson, M., et al., 2017. RNA interference restricts Rift Valley fever virus in multiple insect systems. mSphere 2.

Eberle, M.W., Reisen, W.K., 1986. Studies on autogeny in Culex tarsalis: 1. Selection and genetic experiments. J. Am. Mosq. Control Assoc. 2, 38–43.

Foy, B.D., Myles, K.M., Pierro, D.J., Sanchez-Vargas, I., Uhlirova, M., Jindra, M., Beaty, B.J., Olson, K.E., 2004. Development of a new Sindbis virus transducing system and its characterization in three Culicine mosquitoes and two Lepidopteran species. Insect Mol. Biol. 13, 89–100.

Fragkoudis, R., Ballany, C.M., Boyd, A., Fazakerley, J.K., 2008. In Semliki Forest virus encephalitis, antibody rapidly clears infectious virus and is required to eliminate viral material from the brain, but is not required to generate lesions of demyelination. J. Gen. Virol. 89, 2565–2568.

Frentiu, F.D., Zakir, T., Walker, T., Popovici, J., Pyke, A.T., van den Hurk, A., McGraw, E.A., O'Neill, S.L., 2014. Limited dengue virus replication in field-collected *Aedes aegypti* mosquitoes infected with *Wolbachia*. PLoS Neglected Trop. Dis. 8, e2688.

Fros, J.J., Miesen, P., Vogels, C.B., Gaibani, P., Sambri, V., Martina, B.E., Koenraadt, C.J., van Rij, R.P., Vlak, J.M., Takken, W., et al., 2015. Comparative Usutu and West Nile virus transmission potential by local Culex pipiens mosquitoes in north-western Europe. One Health 1, 31–36.

Göertz, G.P., Fros, J.J., Miesen, P., Vogels, C.B., van der Bent, M.L., Geertsema, C., Koenraadt, C.J., van Rij, R.P., van Oers, M.M., Pijlman, G.P., 2016. Noncoding subgenomic flavivirus RNA is processed by the mosquito RNA interference machinery and determines West Nile virus transmission by *Culex pipiens* mosquitoes. J. Virol. 90, 10145–10159.

Goic, B., Stapleford, K.A., Frangeul, L., Doucet, A.J., Gausson, V., Blanc, H., Schemmel-Jofre, N., Cristofari, G., Lambrechts, L., Vignuzzi, M., et al., 2016. Virus-derived DNA drives mosquito vector tolerance to arboviral infection. Nat. Commun. 7, 12410.

Goic, B., Vodovar, N., Mondotte, J.A., Monot, C., Frangeul, L., Blanc, H., Gausson, V., Vera-Otarola, J., Cristofari, G., Saleh, M.C., 2013. RNA-mediated interference and reverse transcription control the persistence of RNA viruses in the insect model *Drosophila*. Nat. Immunol. 14, 396–403.

Gunawardane, L.S., Saito, K., Nishida, K.M., Miyoshi, K., Kawamura, Y., Nagami, T., Siomi, H., Siomi, M.C., 2007. A slicer-mediated mechanism for repeat-associated siRNA 5' end formation in *Drosophila*. Science 315, 1587–1590.

Hess, A.M., Prasad, A.N., Ptitsyn, A., Ebel, G.D., Olson, K.E., Barbacioru, C., Monighetti, C., Campbell, C.L., 2011. Small RNA profiling of Dengue virus-mosquito interactions implicates the PIWI RNA pathway in anti-viral defense. BMC Microbiol. 11, 45.

Hsu, S.H., Mao, W.H., Cross, J.H., 1970. Establishment of a line of cells derived from ovarian tissue of Culex quinquefasciatus Say. J. Med. Entomol. 7, 703–707.

Keene, K.M., Foy, B.D., Sanchez-Vargas, I., Beaty, B.J., Blair, C.D., Olson, K.E., 2004. RNA interference acts as a natural antiviral response to O'nyong-nyong virus (Alphavirus; Togaviridae) infection of *Anopheles gambiae*. In: Proceedings of the National Academy of Sciences of the United States of America. 101. pp. 17240–17245.

Kilpatrick, A.M., 2011. Globalization, land use, and the invasion of West Nile virus. Science 334, 323–327.

Kim, V.N., Han, J., Siomi, M.C., 2009. Biogenesis of small RNAs in animals. Nat. Rev. Mol. Cell Biol. 10, 126–139.

Lanciotti, R.S., Kerst, A.J., Nasci, R.S., Godsey, M.S., Mitchell, C.J., Savage, H.M., Komar,

N., Panella, N.A., Allen, B.C., Volpe, K.E., et al., 2000. Rapid detection of west nile virus from human clinical specimens, field-collected mosquitoes, and avian samples by a TaqMan reverse transcriptase-PCR assay. J. Clin. Microbiol. 38, 4066–4071.
Langmead, B., Trapnell, C., Pop, M., Salzberg, S.L., 2009. Ultrafast and memory-efficient alignment of short DNA sequences to the human genome. Genome Biol. 10, R25.
Lazear, H.M., Diamond, M.S., 2016. Zika virus: new clinical syndromes and its emergence in the western hemisphere. J. Virol. 90, 4864–4875.
Li, H., Handsaker, B., Wysoker, A., Fennell, T., Ruan, J., Homer, N., Marth, G., Abecasis, G., Durbin, R., 2009. The sequence alignment/map format and SAMtools. Bioinformatics 25, 2078–2079.
Lozano-Fuentes, S., Fernandez-Salas, I., de Lourdes Munoz, M., Garcia-Rejon, J., Olson, K.E., Beaty, B.J., Black, W.C.t., 2009. The neovolcanic axis is a barrier to gene flow among Aedes aegypti populations in Mexico that differ in vector competence for Dengue 2 virus. PLoS Neglected Trop. Dis. 3, e468.
McMeniman, C.J., Lane, R.V., Cass, B.N., Fong, A.W., Sidhu, M., Wang, Y.F., O'Neill, S.L., 2009. Stable introduction of a life-shortening Wolbachia infection into the mosquito *Aedes aegypti*. Science 323, 141–144.
Miesen, P., Girardi, E., van Rij, R.P., 2015. Distinct sets of PIWI proteins produce arbovirus and transposon-derived piRNAs in *Aedes aegypti* mosquito cells. Nucleic Acids Res. 43, 6545–6556.
Miesen, P., Ivens, A., Buck, A.H., van Rij, R.P., 2016. Small RNA profiling in dengue virus 2-infected *Aedes* mosquito cells reveals viral piRNAs and novel host miRNAs. PLoS Neglected Trop. Dis. 10, e0004452.
Morazzani, E.M., Wiley, M.R., Murreddu, M.G., Adelman, Z.N., Myles, K.M., 2012. Production of virus-derived ping-pong-dependent piRNA-like small RNAs in the mosquito soma. PLoS Pathog. 8, e1002470.
Moyes, C.L., Vontas, J., Martins, A.J., Ng, L.C., Koou, S.Y., Dusfour, I., Raghavendra, K., Pinto, J., Corbel, V., David, J.P., et al., 2017. Contemporary status of insecticide resistance in the major Aedes vectors of arboviruses infecting humans. PLoS Neglected Trop. Dis. 11, e0005625.
Myles, K.M., Wiley, M.R., Morazzani, E.M., Adelman, Z.N., 2008. Alphavirus-derived small RNAs modulate pathogenesis in disease vector mosquitoes. In: Proceedings of the National Academy of Sciences of the United States of America. 105. pp. 19938–19943.
Nag, D.K., Brecher, M., Kramer, L.D., 2016a. DNA forms of arboviral RNA genomes are generated following infection in mosquito cell cultures. Virology 498, 164–171.
Nag, D.K., Brecher, M., Kramer, L.D., 2016b. DNA forms of arboviral RNA genomes are generated following infection in mosquito cell cultures. Virology 498, 164–171.
Nag, D.K., Kramer, L.D., 2017. Patchy DNA forms of the Zika virus RNA genome are generated following infection in mosquito cell cultures and in mosquitoes. J. Gen. Virol. 98, 2731–2737.
Nishida, K.M., Saito, K., Mori, T., Kawamura, Y., Nagami-Okada, T., Inagaki, S., Siomi, H., Siomi, M.C., 2007. Gene silencing mechanisms mediated by Aubergine piRNA complexes in Drosophila male gonad. RNA 13, 1911–1922.
Olson, K.E., Higgs, S., Gaines, P.J., Powers, A.M., Davis, B.S., Kamrud, K.I., Carlson, J.O., Blair, C.D., Beaty, B.J., 1996. Genetically engineered resistance to dengue-2 virus transmission in mosquitoes. Science 272, 884–886.
Palatini, U., Miesen, P., Carballar-Lejarazu, R., Ometto, L., Rizzo, E., Tu, Z., van Rij, R.P., Bonizzoni, M., 2017. Comparative genomics shows that viral integrations are abundant and express piRNAs in the arboviral vectors Aedes aegypti and Aedes albopictus. BMC Genomics 18, 512.
Paradkar, P.N., Trinidad, L., Voysey, R., Duchemin, J.B., Walker, P.J., 2012. Secreted Vago restricts West Nile virus infection in *Culex* mosquito cells by activating the Jak-STAT pathway. In: Proceedings of the National Academy of Sciences of the United States of America. 109. pp. 18915–18920.
Poirier, E.Z., Goic, B., Tome-Poderti, L., Frangeul, L., Boussier, J., Gausson, V., Blanc, H., Vallet, T., Loyd, H., Levi, L.I., et al., 2018. Dicer-2-Dependent generation of viral DNA from defective genomes of RNA viruses modulates antiviral immunity in insects. Cell Host Microbe 23, 353–365.
Ramírez, A.L., 2019. Culex quinquefasciatus mosquito. figshare.
Ramirez, J.L., Dimopoulos, G., 2010. The Toll immune signaling pathway control conserved anti-dengue defenses across diverse Ae. aegypti strains and against multiple dengue virus serotypes. Dev. Comp. Immunol. 34, 625–629.
Rückert, C., Bell-Sakyi, L., Fazakerley, J.K., Fragkoudis, R., 2014. Antiviral responses of arthropod vectors: an update on recent advances. Virusdisease 25, 249–260.
Saito, K., Siomi, M.C., 2010. Small RNA-mediated quiescence of transposable elements in animals. Dev. Cell 19, 687–697.
Salimi, H., Cain, M.D., Klein, R.S., 2016. Encephalitic arboviruses: emergence, clinical presentation, and neuropathogenesis. Neurotherapeutics 13, 514–534.
Sanchez-Vargas, I., Travanty, E.A., Keene, K.M., Franz, A.W., Beaty, B.J., Blair, C.D., Olson, K.E., 2004. RNA interference, arthropod-borne viruses, and mosquitoes. Virus Res. 102, 65–74.
Schnettler, E., Donald, C.L., Human, S., Watson, M., Siu, R.W.C., McFarlane, M., Fazakerley, J.K., Kohl, A., Fragkoudis, R., 2013. Knockdown of piRNA pathway proteins results in enhanced Semliki Forest virus production in mosquito cells. J. Gen. Virol. 94, 1680–1689.
Schwarz, D.S., Hutvagner, G., Du, T., Xu, Z., Aronin, N., Zamore, P.D., 2003. Asymmetry in the assembly of the RNAi enzyme complex. Cell 115, 199–208.
Scott, J.C., Brackney, D.E., Campbell, C.L., Bondu-Hawkins, V., Hjelle, B., Ebel, G.D., Olson, K.E., Blair, C.D., 2010. Comparison of dengue virus type 2-specific small RNAs from RNA interference-competent and -incompetent mosquito cells. PLoS Neglected Trop. Dis. 4, e848.
Senti, K.A., Brennecke, J., 2010. The piRNA pathway: a fly's perspective on the guardian of the genome. Trends Genet.: TIG (Trends Genet.) 26, 499–509.
Shi, P.Y., Tilgner, M., Lo, M.K., Kent, K.A., Bernard, K.A., 2002. Infectious cDNA clone of the epidemic west nile virus from New York City. J. Virol. 76, 5847–5856.
Singh, K.R.P., 1967. Cell cultures derived from larvae of Aedes albopictus (skuse) and Aedes aegypti (L). Curr. Sci. India. 36, 506.
Siomi, M.C., Miyoshi, T., Siomi, H., 2010. piRNA-mediated silencing in Drosophila germlines. Semin. Cell Dev. Biol. 21, 754–759.
Siomi, M.C., Sato, K., Pezic, D., Aravin, A.A., 2011. PIWI-interacting small RNAs: the vanguard of genome defence. Nat. Rev. Mol. Cell Biol. 12, 246–258.
Souza-Neto, J.A., Sim, S., Dimopoulos, G., 2009. An evolutionary conserved function of the JAK-STAT pathway in anti-dengue defense. In: Proceedings of the National Academy of Sciences of the United States of America. 106. pp. 17841–17846.
Tassetto, M., Kunitomi, M., Andino, R., 2017. Circulating immune cells mediate a systemic RNAi-based adaptive antiviral response in Drosophila. Cell 169, 314–325 e313.
Travanty, E.A., Adelman, Z.N., Franz, A.W., Keene, K.M., Beaty, B.J., Blair, C.D., James, A.A., Olson, K.E., 2004. Using RNA interference to develop dengue virus resistance in genetically modified Aedes aegypti. Insect Biochem. Mol. Biol. 34, 607–613.
Tsetsarkin, K.A., Chen, R., Weaver, S.C., 2016. Interspecies transmission and chikungunya virus emergence. Curr. Opin. Virol. 16, 143–150.
van Cleef, K.W., van Mierlo, J.T., Miesen, P., Overheul, G.J., Fros, J.J., Schuster, S., Marklewitz, M., Pijlman, G.P., Junglen, S., van Rij, R.P., 2014. Mosquito and Drosophila entomobirnaviruses suppress dsRNA- and siRNA-induced RNAi. Nucleic Acids Res. 42, 8732–8744.
Varjak, M., Donald, C.L., Mottram, T.J., Sreenu, V.B., Merits, A., Maringer, K., Schnettler, E., Kohl, A., 2017a. Characterization of the Zika virus induced small RNA response in Aedes aegypti cells. PLoS Neglected Trop. Dis. 11, e0006010.
Varjak, M., Maringer, K., Watson, M., Sreenu, V.B., Fredericks, A.C., Pondeville, E., Donald, C.L., Sterk, J., Kean, J., Vazeille, M., et al., 2017b. Aedes aegypti Piwi4 is a noncanonical PIWI protein involved in antiviral responses. mSphere 2.
Vasconcelos, P.F., Calisher, C.H., 2016. Emergence of Human Arboviral Diseases in the Americas, 2000-2016. Vector Borne Zoonotic Dis. 16, 295–301.
Vodovar, N., Bronkhorst, A.W., van Cleef, K.W., Miesen, P., Blanc, H., van Rij, R.P., Saleh, M.C., 2012. Arbovirus-derived piRNAs exhibit a ping-pong signature in mosquito cells. PLoS One 7, e30861.
Wang, Y., Jin, B., Liu, P., Li, J., Chen, X., Gu, J., 2018. piRNA Profiling of Dengue Virus Type 2-Infected Asian Tiger Mosquito and Midgut Tissues. Viruses 10.
Watson, M., Schnettler, E., Kohl, A., 2013. viRome: an R package for the visualization and analysis of viral small RNA sequence datasets. Bioinformatics 29, 1902–1903.
Weaver, S.C., Costa, F., Garcia-Blanco, M.A., Ko, A.I., Ribeiro, G.S., Saade, G., Shi, P.Y., Vasilakis, N., 2016. Zika virus: history, emergence, biology, and prospects for control. Antivir. Res. 130, 69–80.
Weaver, S.C., Reisen, W.K., 2010. Present and future arboviral threats. Antivir. Res. 85, 328–345.
Weger-Lucarelli, J., Rückert, C., Grubaugh, N.D., Misencik, M.J., Armstrong, P.M., Stenglein, M.D., Ebel, G.D., Brackney, D.E., 2018. Adventitious viruses persistently infect three commonly used mosquito cell lines. Virology 521, 175–180.
Winskill, P., Carvalho, D.O., Capurro, M.L., Alphey, L., Donnelly, C.A., McKemey, A.R., 2015. Dispersal of engineered male Aedes aegypti mosquitoes. PLoS Neglected Trop. Dis. 9, e0004156.
Xi, Z., Ramirez, J.L., Dimopoulos, G., 2008. The Aedes aegypti toll pathway controls dengue virus infection. PLoS Pathog. 4, e1000098.